Bright, dark, antidark, and kink solitons in media with periodically alternating sign of nonlinearity

Yannis Kominis
School of Electrical and Computer Engineering, National Technical University of Athens, Zographou GR-15773, Greece
and Department of Mathematics, University of Patras, Patras GR-26500, Greece
(Received 13 May 2013; published 28 June 2013)

The formation of solitary waves (SW) in media with periodically alternating sign of nonlinearity is investigated under a geometrical phase space approach. It is shown that a remarkably rich set of all types of SW, including bright, dark, antidark, and kink solitons is supported by this type of structure. The existence conditions of all SW are systematically defined in the parameter space of the system and their propagation dynamics are investigated through numerical simulations.

DOI: 10.1103/PhysRevA.87.063849 PACS number(s): 42.65.Tg, 42.65.Jx, 42.65.Sf, 03.75.Lm

I. INTRODUCTION

Spatial self-localization of waves in nonlinear periodic structures is a ubiquitous phenomenon resulting from the interplay between the medium inhomogeneity and nonlinearity that has no analog in homogeneous media. Its effect gives rise to the existence of a rich set of solitary waves (SW) in a large variety of physical systems. Among them, the formation and propagation of light SW in photonic structures such as optical lattices and waveguide arrays are widely studied in the context of nonlinear optics [1–4], whereas matter SW are studied in the context of Bose-Einstein condensates (BEC) [5–8], with theoretical studies on both fields progressing in parallel due to common underlying models of wave propagation.

In general, SW have the form of a spatially localized transition between two asymptotic states. Different types of SW can be characterized on the basis of their asymptotic states, with bright solitons having zero asymptotic states, dark (antidark) solitons having nonzero asymptotic states of opposite (same) sign, and kink solitons having asymptotic states with different values in general. The existence of such SW is closely related to complex dynamics of the system describing the spatial wave profile formation with the respective asymptotic states having the form of hyperbolic plane-wave solutions of the system. From a geometrical point of view, in the phase space of the system, SW can be found as intersections of the invariant stable and unstable manifolds of the hyperbolic solutions corresponding to their asymptotic states [9].

Among the different types of SW, bright solitons have been most extensively theoretically studied and experimentally demonstrated in several configurations with varying degree of spatial complexity ranging from monochromatic modulation of the linear refractive index to superlattices and nonperiodic structures. Due to the presence of the inhomogeneity, bright solitons can be formed in either focusing or defocusing media, in contrast to the homogeneous case [10]. Theoretical studies have been based either on continuous models consisting of the nonlinear Schrödinger (NLS) equation with spatially varying coefficients [11–13] or simplified discrete models under the tight-binding approximation describing deeply trapped narrow SW [4]. Dark solitons have been theoretically studied in both discrete [14] and continuous models [15] and their existence has been shown in various configurations.

Antidark as well as kink solitons have been less intensively studied than dark and bright solitons. Antidark solitons have been theoretically studied in continuous vector two-component models describing either weakly trapped SW in band gap photonic structures with the utilization of coupled mode theory [16,17] or in binary Bose-Einstein condensates [18,19]. Discrete binary models describing waveguide arrays with alternating positive-negative couplings have also been shown to support antidark soliton solutions [20,21]. Kink solitons (also referred to as shocks or domain walls) in periodic structures have been considered mostly in discrete models [21–23] as well as in coupled wave equations describing vector SW [24,25]. The formation of surface SW having the form of kink solitons has also been studied in nonperiodic structures consisting either of interfaces between lattices [26–28] or localized modulations of the medium [29,30]. In the latter case the SW profile asymmetry is directly enforced by the nonperiodic spatial modulation of the medium in contrast to the former case of periodic modulations where the profile asymmetry results from the dynamical interplay between the nonlinearity and the periodicity of the medium.

Structures of increasing complexity of the spatial modulation of the medium have also been considered from the point of view of engineering the inhomogeneity in order to provide desirable properties of SW formation and propagation dynamics. Among them, a large amount of work has been focused on media where, in addition to the linear properties, the nonlinearity is also transversely modulated forming nonlinear lattices [13,31,32]. In such structures both the strength and the sign of the nonlinearity can vary across their transverse dimension. A periodic alternation of the sign of the nonlinear refractive index corresponds to a periodically focusing and defocusing optical medium in the context of nonlinear optics, whereas in the context of BEC the periodic alternation of the sign of the scattering length corresponds to periodically repulsive and attractive interactions between the atoms [32]. Layered structures combining piecewise constant profiles of the linear and nonlinear properties of the medium are usually referred to as Kronig-Penney (KP) lattices and have been considered in terms of SW formation and propagation [33–35].

In this work, a layered medium with periodically alternating sign of nonlinearity is considered. The continuous model of the NLS equation with piecewise constant coefficients of the linear and nonlinear terms is utilized to describe wave propagation under no restriction as those implied by the tight-binding approximation or the coupled-mode approach. A geometrical phase space analysis reveals the remarkable richness of all

types of SW that can be supported by such structures, including bright, dark, antidark, and kink solitons as well as bound states. The propagation dynamics of these SW are investigated with the utilization of numerical simulations.

II. MODEL

Wave propagation in a nonlinear inhomogeneous medium is governed by the NLS equation with transversely varying coefficients

$$i\psi_z + \psi_{xx} + n(x)\psi + 2s(x)|\psi|^2\psi = 0. \tag{1}$$

We consider the case of a periodic slab structure consisting of alternating focusing and defocusing layers [as shown in Fig. 1(a)] with the linear refractive index and nonlinearity varying as

$$[n(x),s(x)] = \begin{cases} [n_F,1], & 0 < \mathrm{mod}(x,L) \leqslant L_F \\ [n_{DF},-1], & L_F < \mathrm{mod}(x,L) \leqslant L, \end{cases} \tag{2}$$

where n_F and n_{DF} are the values of the linear refractive index in focusing and defocusing layers, respectively. The widths of the layers are L_F and L_{DF} and the spatial period of the structure is $L = L_F + L_{DF}$.

Stationary wave solutions of Eq. (1) have the form

$$\psi(x,z) = u(x)\exp(ik_z z) \tag{3}$$

with k_z being the propagation constant, and are given from the equation

$$u_{xx} + [n(x) - k_z]u + 2s(x)u^3 = 0 \tag{4}$$

corresponding to a nonautonomous dynamical system. This system is nonintegrable and describes chaotic dynamics for the transverse wave profile formation. The dynamics can be studied in the three-dimensional extended phase space of the system consisting of (u,u_x,x) by utilizing Poincaré surfaces of section at $x = mL$, with m integer, due to the periodicity of the x dependence. The respective Poincaré map has a fixed point at the origin O of the plane (u,u_x), corresponding to a constant zero solution $u_0 = 0$. An additional pair of fixed points, corresponding to nonzero constant solutions $u_0 \neq 0$, exists when

$$k_z = \frac{n_{DF} + n_F}{2} \equiv \bar{n}. \tag{5}$$

The amplitude u_0 of such solutions is given by

$$u_0^2 = \frac{n_{DF} - n_F}{4} \equiv \frac{\Delta n}{4} \tag{6}$$

and the corresponding fixed points $P_\pm$ of the Poincaré map are located at $(u,u_x) = (\pm\sqrt{\Delta n}/2,0)$. The condition for the existence of these fixed points is that the value of the linear refractive index in the defocusing layers is greater than the value of the linear refractive index in the defocusing layers ($n_{DF} > n_F$). In such case a high value of the linear refractive index can counterbalance the effect of the nonlinear reduction of the refractive index inside a defocusing layer, whereas the opposite holds for a focusing layer. Therefore, interesting dynamics of the system (4) are expected as a result of the interplay between these two mechanisms. The stability type of the fixed points $O, P_\pm$ can be determined by linearizing Eq. (4) resulting in

$$q_{xx} + s(x)\left(-\frac{\Delta n}{2} + 6u_0^2\right)q = 0, \tag{7}$$

where q is the first-order variation around the solutions corresponding to $O, P_\pm$. This is a linear periodic system having solutions that satisfy the Bloch periodicity condition

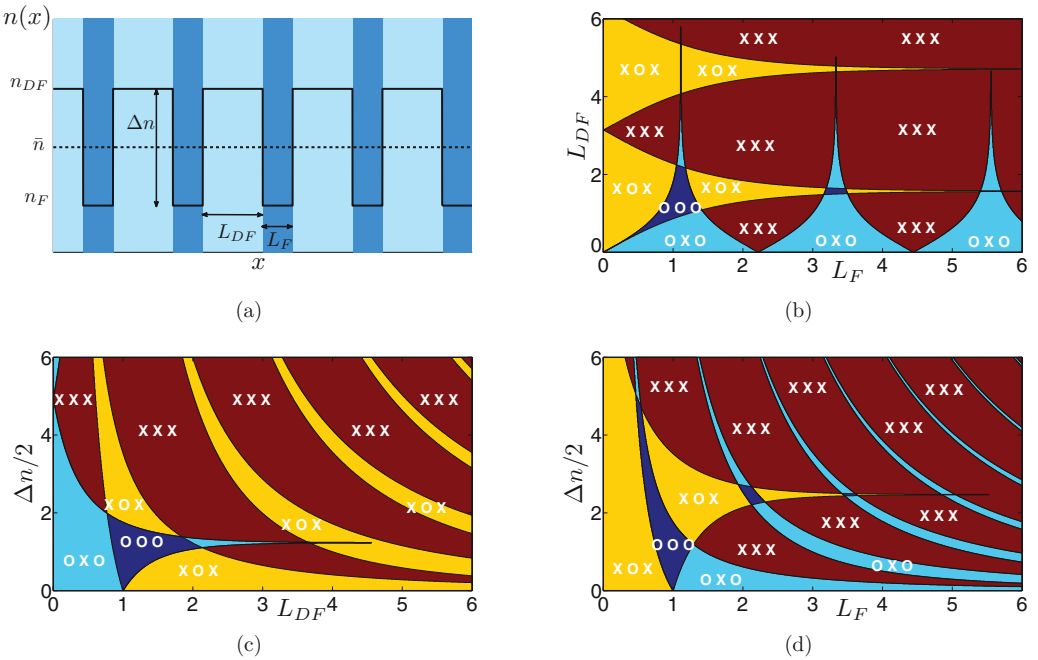

FIG. 1. (Color online) (a) Transverse profile of the structure and variation of the linear refractive index. Blue (dark) and (light) cyan regions denote focusing and defocusing layers. (b)–(d) Parametric space regions with different stability type of the fixed points P_-, O, P_+ with "X" and "O" denoting a saddle and a center, respectively. (b) $\Delta n/2 = 1$, (c) $L_F = 1$, and (d) $L_{DF} = 1$.

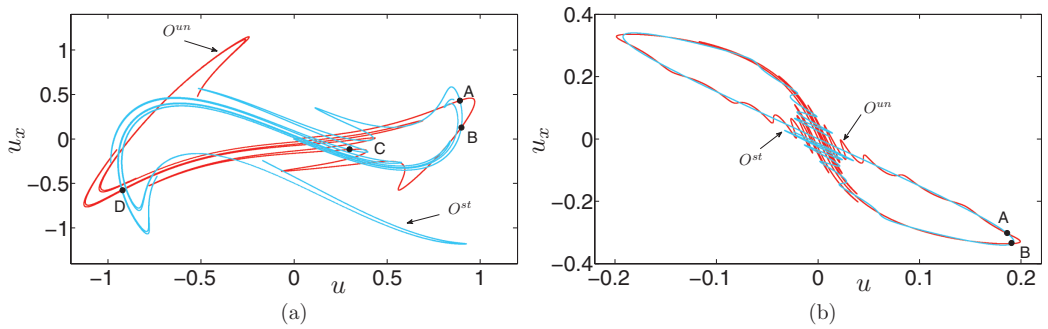

FIG. 2. (Color online) Branches of the stable O^{st} (blue) and unstable O^{un} (red) manifolds of O in a Poincare surface of section. Black dots denote intersections of the manifolds. (a) $L_F = 1$, $L_{DF} = 0.5$, $\Delta n/2 = 1$, (b) $L_F = 1$, $L_{DF} = 2.15$, $\Delta n/2 = 1.2$. Both parameter sets correspond to "O X O" cases.

$q(x + L) = \exp(ipx)q(x)$ with $p \in [-\pi/L, \pi/L]$ being the respective Floquet exponent. Using continuity of u and u_x at the boundaries of the layers we obtain

$$\cos(pL) = \cos(\sqrt{a_i}L_F)\cos(\sqrt{-a_i}L_{DF}) \equiv \Delta, \quad i = O, P_{\pm} \tag{8}$$

with $a_O = -\Delta n/2$ and $a_{P_\pm} = 2\Delta n$ for the two fixed-point solutions, respectively. Floquet exponents p obtained from Eq. (8) have a zero imaginary part when $\Delta \leqslant 1$ corresponding to stable solutions, while they have a nonzero imaginary part when $\Delta > 1$ corresponding to unstable solutions. The respective fixed points of the Poincaré map correspond to centers and saddles. Therefore, the function $\Delta = \Delta(L_F, L_{DF}, \Delta n)$ determines the stability of the constant solutions of zero and nonzero amplitude in terms of the geometrical and material properties of the structure. In Figs. 1(b)–1(d), the dependence of the stability type of O and $P_\pm$ on the parameters of the structure is illustrated. Four different combinations, labeled as "O O O," "O X O," "X O X," and "X X X," can take place in the parameter space, with "O" denoting a stable (center) and "X" denoting an unstable (saddle) fixed point and the relative position of the symbols corresponding to the fixed-point order "P_- O P_+." As expected, $L_F \gg L_{DF}$ ($L_F \ll L_{DF}$) corresponds to "O X O" ("X O X"), since focusing (defocusing) dominates across the structure. Comparable widths of the focusing and defocusing layers additionally allow for cases corresponding to "X X X" as well as "O O O," since the interplay between the two competing mechanisms of nonlinear focusing and defocusing can alter the type of stability of one of the fixed points. The result of this interplay depends not only on the relative widths of the focusing and defocusing layers, as shown in Fig. 1(b), but it also depends crucially on the difference of the linear refractive index (Δn) between the layers, as shown in Figs. 1(c) and 1(d).

III. SOLITARY WAVES

Stationary solitary wave solutions of Eq. (1) correspond to solutions of Eq. (4) with constant asymptotic values.

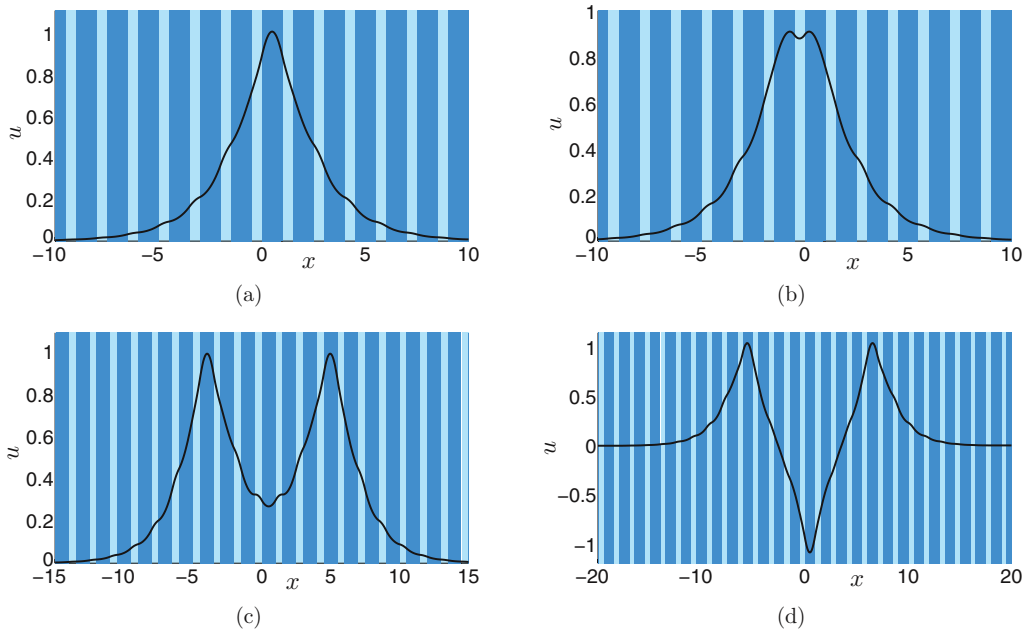

FIG. 3. (Color online) Bright soliton profiles corresponding to points A (a), B (b), C (c), and D (d) of Fig. 2(a).

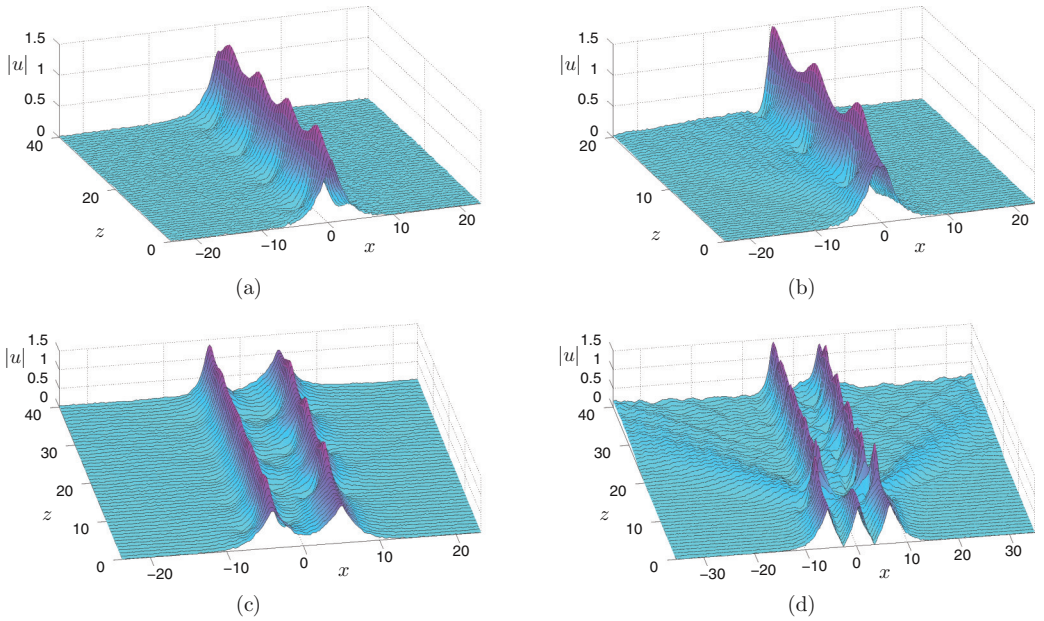

FIG. 4. (Color online) Propagation of bright solitons with profiles shown in Fig. 3.

Therefore, the existence of solitary waves is directly related to the existence of constant solutions of Eq. (4) that are saddle points of the respective Poincaré map. Solitary waves correspond to orbits connecting a saddle point either to itself (homoclinic orbits) or to another saddle point (heteroclinic orbits). These orbits are located within both the two-dimensional stable and unstable manifolds of the same or different saddle points and can be found as intersections of these manifolds in the three-dimensional extended phase space of system (4). In the Poincaré surface of section, the traces of these orbits are found as points of intersection between the curves corresponding to the intersection between the Poincaré surface of section and the respective stable and unstable manifolds, namely, homoclinic or heteroclinic points [9,13]. Solitary wave solutions can be found by utilizing standard techniques for solving boundary-value problems [36]. In this work, the aforementioned geometrical approach is adopted, so that the problem of finding stationary SW solutions is replaced with the problem of finding intersection points between two invariant curves. This method not only provides accurate solitary wave solutions but it also allows for an overview of solution families existing for each parameter set and provides physical understanding of the underlying mechanisms of solitary wave formation.

The stationary solitary waves can be either stable or unstable under propagation. A necessary condition for their stability is that the respective background corresponding to constant zero or nonzero solutions is modulationally stable. It is well known [37] that for a self-focusing nonlinearity only the zero background is modulationally stable, while for a self-defocusing nonlinearity both zero and nonzero backgrounds are modulationally stable. In a structure with alternating sign of nonlinearity it is expected that modulational stability or instability is a result of the interplay between the two competing mechanisms analogously to cases of discrete binary models [21]. In order to focus on the propagation stability of solitary waves having various profiles, we consider cases where the respective background solutions are modulationally stable. In the following propagation simulations a noise level of the order of 1% with respect to the soliton amplitude has been superimposed in order to confirm modulational stability of nonzero backgrounds and investigate soliton stability.

A. Bright solitons

Bright solitons have zero asymptotic values and correspond to orbits homoclinic to the fixed point O at the origin, which has to be a saddle point. In Fig. 2(a) the intersection of

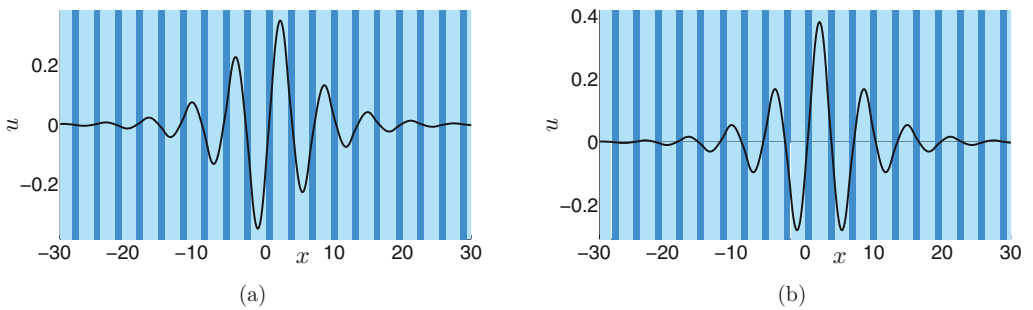

FIG. 5. (Color online) Bright soliton profiles corresponding to points A (a) and B (b) of Fig. 2(b).

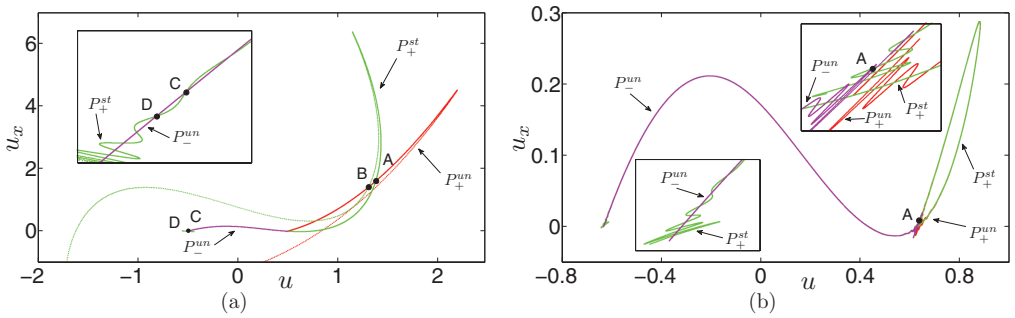

FIG. 6. (Color online) Branches of the stable P_+^{st} (green), unstable P_+^{un} (red) manifolds of P_+ and the unstable P_-^{un} manifold (magenta) of P_- in a Poincare surface of section. Black dots denote intersections of the manifolds. The insets show details close to the fixed points. (a) $L_F = 0.5$, $L_{DF} = 1$, $\Delta n/2 = 0.5$, (b) $L_F = 0.7$, $L_{DF} = 1$, $\Delta n/2 = 0.8$. Both parameter sets correspond to "X O X" cases.

the stable and unstable manifolds of O with the Poincaré surface of section are shown, for a parameter set $(L_F, L_{DF}, \Delta n)$ corresponding to an "O X O" case. Note that, due to symmetry, only one branch of the manifolds is shown. The respective curves intersect transversely at several sequences of points, with each sequence corresponding to a different bright soliton profile. Fundamental soliton profiles corresponding to points A and B of Fig. 2(a) are symmetric with respect to the center of the focusing and the defocusing layers as shown in Figs. 3(a) and 3(b). Their propagation dynamics show that the first soliton that is symmetric with respect to the focusing layer propagates in a stable fashion, undergoing periodic amplitude and width oscillations [Fig. 4(a)], whereas the second soliton initially transforms to the first and then propagates as such [Fig. 4(b)].

More complex bright solitons correspond to intersections of the homoclinic tangles formed by the respective stable and unstable manifolds and consist of multihump profiles as those shown in Figs. 3(c) and 3(d) corresponding to points C and D of Fig. 2(a), respectively. These cases can be considered as bound states composed of combinations of fundamental solitons separated by a finite distance and appropriately matched. It is worth mentioning that the phase space geometrical approach for the study of solitary wave formation provides a clear view of the conditions of existence of such solitons as well as a method for their systematic categorization as intersection points between two invariant curves. Oscillatory propagation of a bound state consisting of a pair of solitons that are symmetric with respect to the center of the focusing layer [profile shown in Fig. 3(c)] is shown in Fig. 4(c), whereas a bound state consisting of two such in-phase solitons separated by an out-of-phase such soliton [profile shown in Fig. 3(d)] evolves to an oscillatory two-soliton bound state under propagation as shown in Fig. 4(d).

Depending on the topology of the stable and unstable manifolds, bipolar bright solitons can also occur for cases as that of Fig. 2(b). Bright soliton profiles being symmetric with respect to the center of the focusing and the defocusing layers correspond to points A and B and are shown in Figs. 5(a) and 5(b). All bright solitons considered here correspond to cases where the origin O is the only saddle point, namely, "O X O" cases; however, as will be shown in the following, bright solitons can also exist in "X X X" cases.

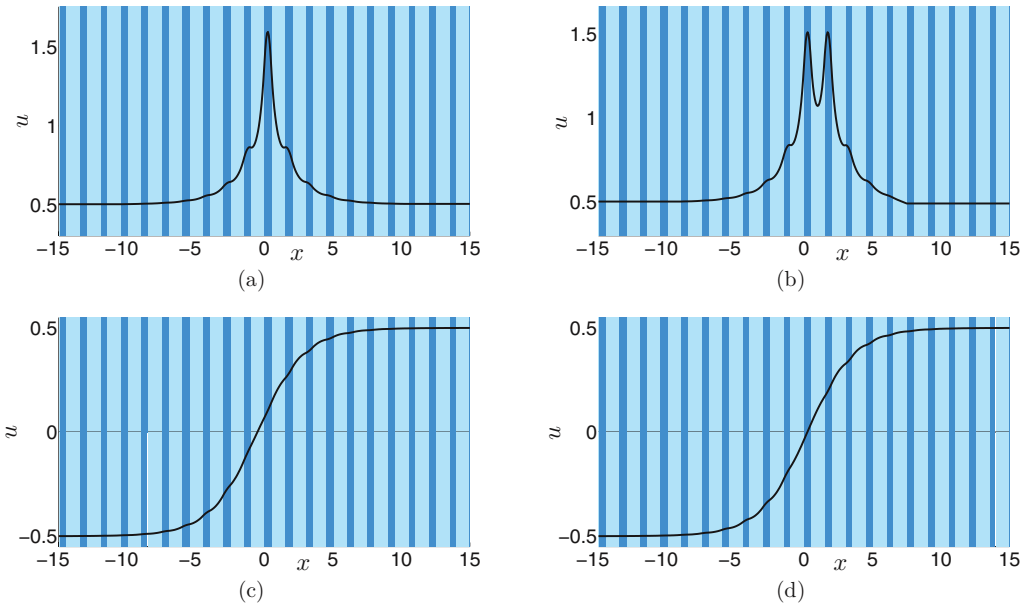

FIG. 7. (Color online) Antidark [(a),(b)] and dark [(c),(d)] soliton profiles corresponding to points A (a), B (b), C (c), and D (d) of Fig. 6(a).

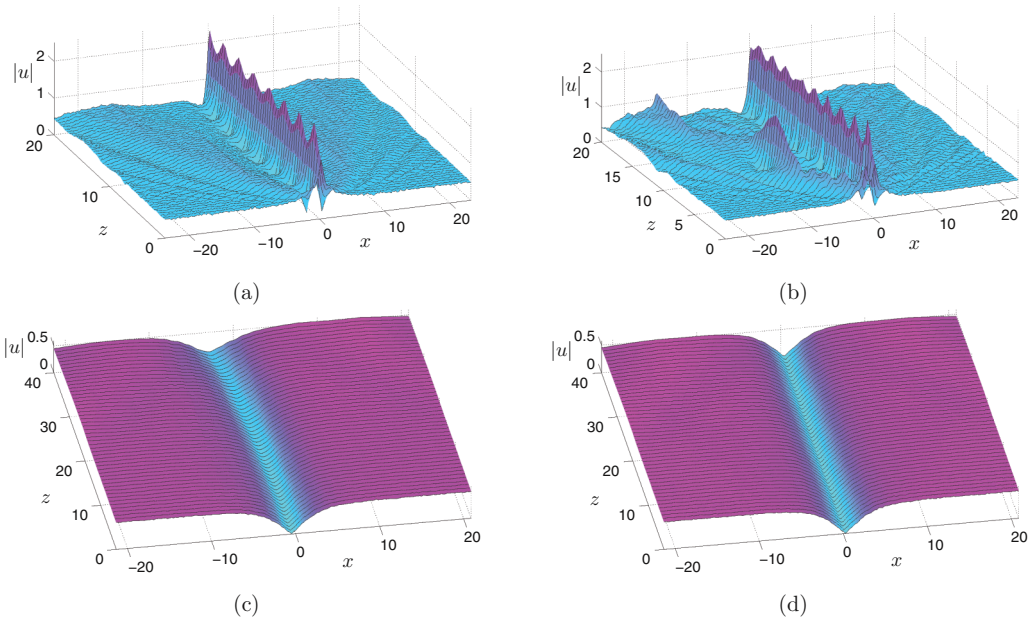

FIG. 8. (Color online) Propagation of antidark and dark solitons with profiles shown in Fig. 7.

B. Dark and antidark solitons

Dark and antidark solitons lay on a constant background and have nonzero asymptotic values. Their existence depends on the existence of nonzero saddle fixed points and on the intersections between branches of the respective stable and unstable manifolds. In Fig. 6(a) branches of the stable and unstable manifolds of P_+ and P_- along with their intersections are shown, for a parameter set corresponding to an "X O X" case. Note that due to symmetry not all branches are shown. Antidark soliton profiles correspond to intersections between the stable and unstable manifold of the same fixed point. Points A and B of Fig. 6(a) correspond to orbits homoclinic to P_+ with the respective transverse profiles depicted in Figs. 7(a) and 7(b) as antidark solitons having profiles that are symmetric with respect to the center of the focusing and defocusing layers. Figure 8(a) shows that the first antidark soliton undergoes stable (oscillatory) propagation, whereas the second antidark soliton transforms to the first one, after emitting a secondary wave that travels transversely across the structure and decays to radiation, as shown in Fig. 8(b).

Heteroclinic points, where the invariant manifolds of the two different fixed points P_- and P_+ intersect, correspond to dark solitons. Dark soliton profiles corresponding to points C and D of Fig. 6(a) are shown in Figs. 7(c) and 7(d). These dark solitons are antisymmetric with respect to the center of the defocusing and the focusing layers. The former undergo an instability due to which they leave the layer where they were originally centered and start traveling across the layers until they are eventually transformed, through radiation emission, in their stable counterpart centered in a different layer, whereas the latter are stable, as shown in Figs. 8(c) and 8(d), respectively.

Bound states composed of the same or different types of solitons can also be found corresponding to intersections between the various branches of the invariant manifolds of the saddle points. The intersection of one branch of the unstable manifold of P_- with a branch of the stable manifold of P_+ depicted by point A in Fig. 6(b) corresponds to a bound state consisting of a dark and an antidark soliton, as shown in Fig. 9(a). Propagation dynamics of such a bound state is depicted in Fig. 9(b) where it is shown that, after an initial stage where the antidark part of the wave evolves to a different antidark wave, a bound state with an oscillatory antidark part emerges. The cases of dark and antidark solitons shown here correspond to parameter regions denoted as "X O X" in Fig. 1;

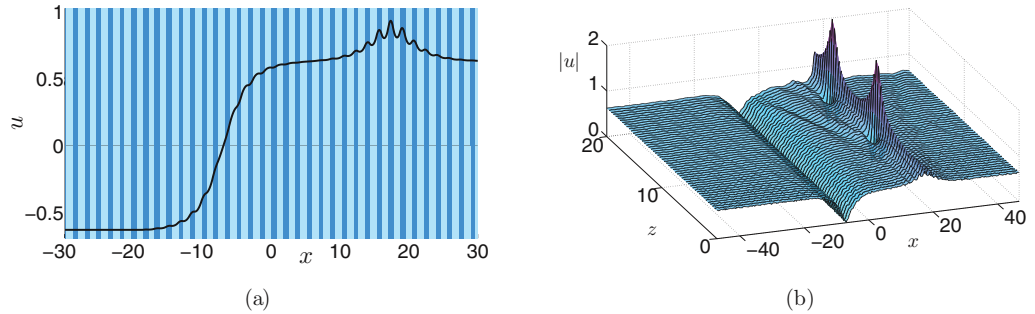

FIG. 9. (Color online) Profile (a) and propagation (b) of composite solitary wave corresponding to point A of Fig. 6(b).

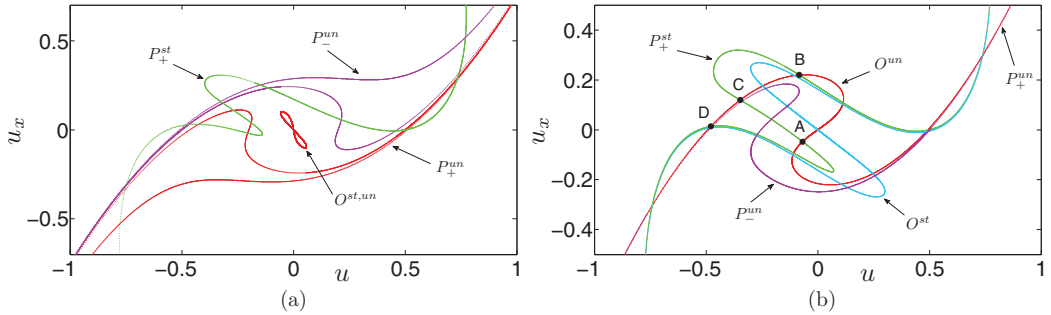

FIG. 10. (Color online) Branches of the stable P_+^{st} (green), unstable P_+^{un} (red) manifolds of P_+, the unstable P_-^{un} manifold (magenta) of P_- and the stable O^{st} (blue), O^{un} unstable (red) manifolds of O in a Poincare surface of section. Black dots denote intersections of the manifolds. (a) $L_F = 1$, $L_{DF} = 4.5$, $\Delta n/2 = 0.5$, (b) $L_F = 1$, $L_{DF} = 3.6$, $\Delta n/2 = 0.5$. Both parameter sets correspond to "X X X" cases.

however, these types of solitons can also be found in cases where not only $P_\pm$ but also the origin O is a saddle, namely, cases "X X X."

C. Kink solitons

Kink solitons are asymmetric solitary waves corresponding to orbits connecting a saddle at the origin O with a saddle at P_+ or P_-. Therefore kink solitons can be found in parameter regions denoted as "X X X" in Fig. 1 and are related to heteroclinic points where invariant manifolds of O and $P_\pm$ intersect. However, as shown in Fig. 10(a), it is possible that invariant manifolds of the origin do not intersect with invariant manifolds of the nonzero fixed points. In such cases bright solitons coexist with dark and antidark solitons but the existence of kink solitons is precluded.

In the most common case, where all invariant manifolds intersect with each other, all types of solitons, including kinks, coexist. Such a case is depicted in Fig. 10(b) where branches of the invariant manifolds (not all of them due to symmetry) are shown. Points A, B, C, and D denote intersections between the unstable manifold of the origin O and the stable manifold of P_+ with the respective profiles shown in Fig. 11. These profiles have no symmetry with respect to the underlying layered structure. Stable propagation is shown in Figs. 12(a) and 12(c), whereas oscillatory propagation is shown in Fig. 12(b). A case of unstable propagation is depicted in Fig. 12(d) where the small amplitude part of the wave propagates in a stable fashion, whereas the part of the wave close to the nonzero background undergoes more complex dynamics.

IV. SUMMARY AND CONCLUSIONS

A periodic layered structure with piecewise constant linear refractive index and alternating sign of nonlinearity has been considered in terms of solitary wave formation and propagation. A detailed analysis of the dynamical system governing the transverse profile of the wave has been utilized in order to identify parameter space regions where saddle points corresponding to plane-wave solutions exist. The various

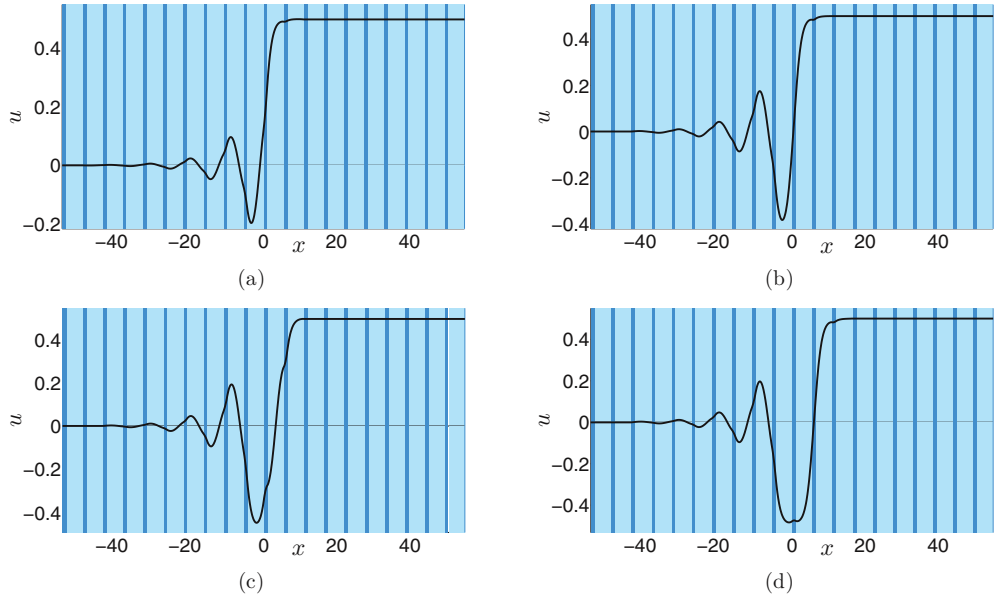

FIG. 11. (Color online) Kink soliton profiles corresponding to points A (a), B (b), C (c), and D (d) of Fig. 10(b).

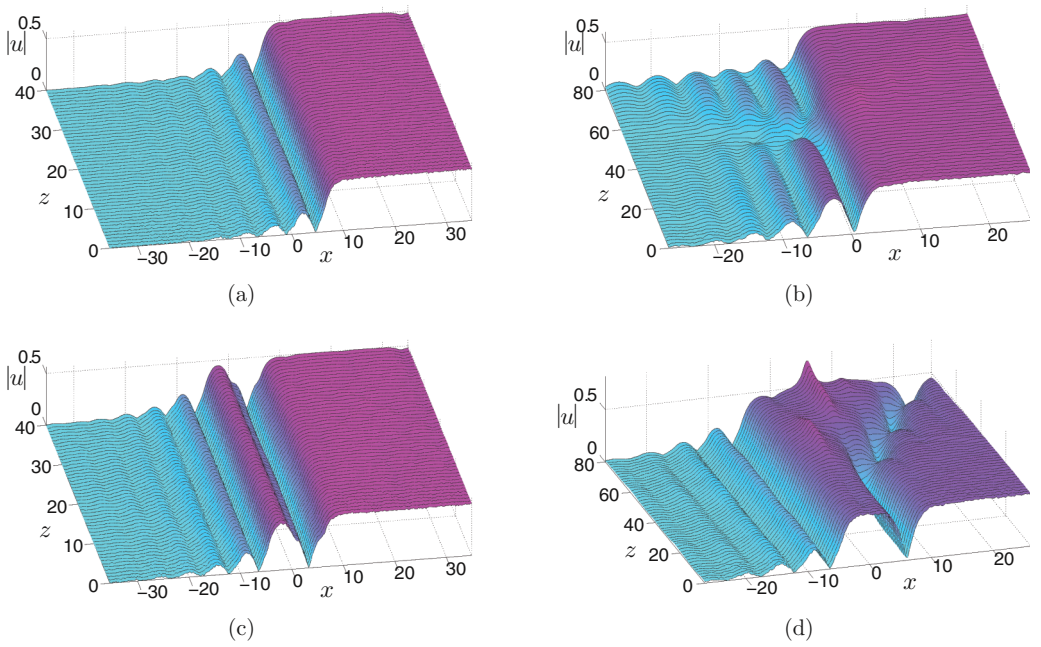

FIG. 12. (Color online) Propagation of kink solitons with profiles shown in Fig. 11.

types of SW are localized transitions between the same or different asymptotic plane-wave backgrounds and can be found as solutions of this dynamical system corresponding to intersections of invariant stable and unstable manifolds of the respective saddles in the phase space. The phase space analysis allows for the systematic investigation of the existence conditions of SW. It is shown that all types of SW, including bright, dark, antidark, and kink solitons as well as bound states can exist in different parameter space regions, while in the greater part of the parameter space they actually coexist. Propagation dynamics of the SW have been investigated with the utilization of numerical simulations and a rich set of dynamical features has been shown including stable and unstable SW propagation and mode transformation. The remarkable richness of all types of SW supported by this class of periodic structures along with its relatively simple periodic form provides intuition in understanding SW formation and is very promising for realistic experiments and applications.

ACKNOWLEDGMENTS

This work has been supported by the Research Project NWDCCPS implemented within the framework of the Action "Supporting Postdoctoral Researchers" of the Operational Program "Education and Lifelong Learning" (Actions Beneficiary: General Secretariat for Research and Technology), and is co-financed by the European Social Fund and the Greek State.

[1] D. N. Christodoulides and R. I. Joseph, Opt. Lett. **13**, 794 (1988).
[2] H. S. Eisenberg, Y. Silberberg, R. Morandotti, A. R. Boyd, and J. S. Aitchison, Phys. Rev. Lett. **81**, 3383 (1998).
[3] D. N. Christodoulides, F. Lederer, and Y. Silberberg, Nature (London) **424**, 817 (2003).
[4] F. Lederer, G. I. Stegeman, D. N. Christodoulides, G. Assanto, M. Segev, and Y. Silberberg, Phys. Rep. **463**, 1 (2008).
[5] S. Burger, K. Bongs, S. Dettmer, W. Ertmer, K. Sengstock, A. Sanpera, G. V. Shlyapnikov, and M. Lewenstein, Phys. Rev. Lett. **83**, 5198 (1999).
[6] A. Trombettoni and A. Smerzi, Phys. Rev. Lett. **86**, 2353 (2001).
[7] F. Kh. Abdullaev, B. B. Baizakov, S. A. Darmanyan, V. V. Konotop, and M. Salerno, Phys. Rev. A **64**, 043606 (2001).
[8] L. Khaykovich, F. Schreck, G. Ferrari, T. Bourdel, J. Cubizolles, L. D. Carr, Y. Castin, and C. Salomon, Science **296**, 1290 (2002).
[9] J. Guckenheimer and P. Holmes, *Nonlinear Oscillations, Dynamical Systems, and Bifurcations of Vector Fields* (Springer-Verlag, Berlin, 1983).
[10] Y. S. Kivshar, Opt. Lett. **18**, 1147 (1993).
[11] N. K. Efremidis and D. N. Christodoulides, Phys. Rev. A **67**, 063608 (2003).
[12] P. J. Y. Louis, E. A. Ostrovskaya, C. M. Savage, and Y. S. Kivshar, Phys. Rev. A **67**, 013602 (2003).
[13] Y. Kominis and K. Hizanidis, Opt. Express **16**, 12124 (2008).
[14] Y. S. Kivshar, W. Krolikowski, and O. A. Chubykalo, Phys. Rev. E **50**, 5020 (1994).
[15] P. J. Y. Louis, E. A. Ostrovskaya, and Y. S. Kivshar, J. Opt. B: Quantum Semiclassical Opt. **6**, S309 (2004).
[16] C. Conti and S. Trillo, Phys. Rev. E **64**, 036617 (2001).
[17] A. V. Yulin and D. V. Skryabin, Phys. Rev. A **67**, 023611 (2003).
[18] P. G. Kevrekidis, H. E. Nistazakis, D. J. Frantzeskakis, B. A. Malomed, and R. Carretero-Gonzalez, Eur. Phys. J. D **28**, 181 (2004).
[19] F. Kh. Abdullaev, A. Gammal, M. Salerno, and L. Tomio, Phys. Rev. A **77**, 023615 (2008).
[20] N. K. Efremidis, P. Zhang, Z. Chen, D. N. Christodoulides, C. E. Ruter, and D. Kip, Phys. Rev. A **81**, 053817 (2010).

[21] M. Conforti, C. De Angelis, and T. R. Akylas, Phys. Rev. A **83**, 043822 (2011); M. Conforti, C. De Angelis, T. R. Akylas, and A. B. Aceves, *ibid.* **85**, 063836 (2012); A. Auditore, M. Conforti, C. De Angelis, and A. B. Aceves, Opt. Commun. **297**, 125 (2013).

[22] S. Darmanyan, A. Kobyakov, F. Lederer, and L. Vazquez, Phys. Rev. B **59**, 5994 (1999); S. Darmanyan, A. Kobyakov, and F. Lederer, JETP **93**, 429 (2001).

[23] R. Noskov, P. Belov, and Y. Kivshar, Sci. Rep. **2**, 873 (2012).

[24] S. Coen and M. Haelterman, Phys. Rev. Lett. **87**, 140401 (2001).

[25] N. Dror, B. A. Malomed, and J. Zeng, Phys. Rev. E **84**, 046602 (2011).

[26] Y. V. Kartashov, V. A. Vysloukh, and L. Torner, Opt. Express **14**, 12365 (2006).

[27] Y. Kominis, A. Papadopoulos, and K. Hizanidis, Opt. Express **15**, 10041 (2007).

[28] C. Huang, J. Zheng, S. Zhong, and L. Dong, Opt. Commun. **284**, 4225 (2011); S. Zhong, C. Huang, C. Li, and L. Dong, *ibid.* **285**, 3674 (2012).

[29] F. Ye, Y. V. Kartashov, V. A. Vysloukh, and L. Torner, Opt. Lett. **32**, 1288 (2008).

[30] Y. V. Kartashov, V. E. Lobanov, B. A. Malomed, and L. Torner, Opt. Lett. **37**, 5000 (2012).

[31] H. Sakaguchi and B. A. Malomed, Phys. Rev. E **72**, 046610 (2005); Phys. Rev. A **81**, 013624 (2010).

[32] Y. V. Kartashov, B. A. Malomed, and L. Torner, Rev. Mod. Phys. **83**, 247 (2011).

[33] Y. Kominis, Phys. Rev. E **73**, 066619 (2006); Y. Kominis and K. Hizanidis, Opt. Lett. **31**, 2888 (2006); Y. Kominis and T. Bountis, Int. J. Bifurcation Chaos **20**, 509 (2010).

[34] T. Mayteevarunyoo and B. A. Malomed, J. Opt. Soc. Am. B **25**, 1854 (2008).

[35] A. S. Rodrigues, P. G. Kevrekidis, M. A. Porter, D. J. Frantzeskakis, P. Schmelcher, and A. R. Bishop, Phys. Rev. A **78**, 013611 (2008).

[36] J. Yang, *Nonlinear Waves in Integrable and Nonintegrable Systems* (SIAM, Philadelphia, 2010).

[37] V. I. Karpman and E. M. Krushkal, Sov. Phys. JETP **28**, 277 (1969).